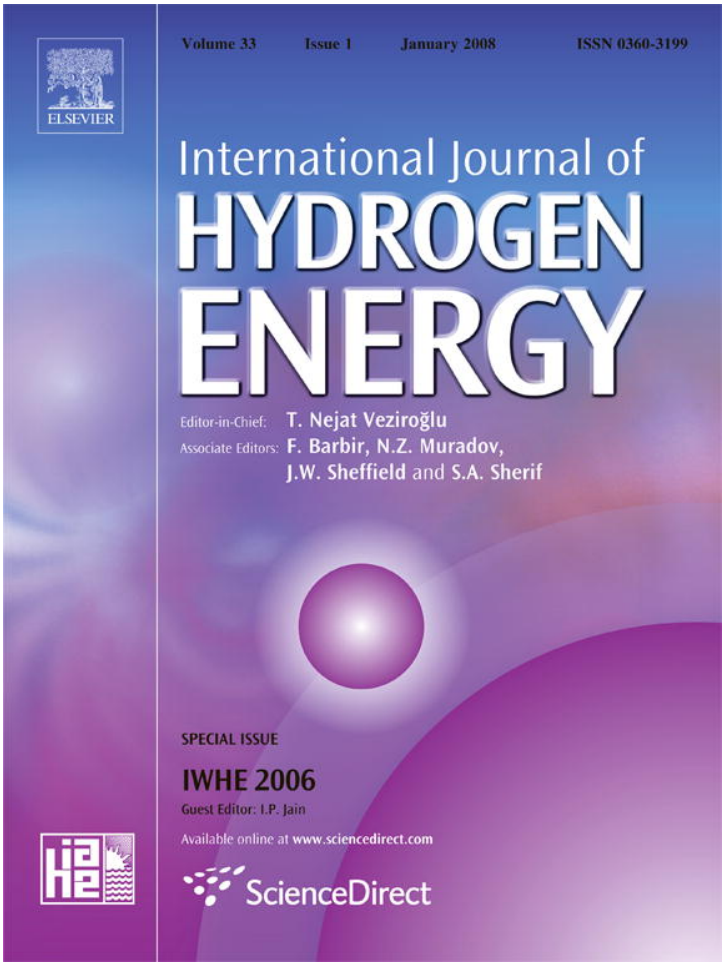

Available online at www.sciencedirect.com
ScienceDirect
International Journal of Hydrogen Energy 33 (2008) 105–110
International Journal of HYDROGEN ENERGY
www.elsevier.com/locate/ijhydene

A DFT study of adsorption hydrogen on the Li-FAU zeolite

Lihua Kang[a], Weiqiao Deng[b], Keli Han[a,*], Tao Zhang[c], Zhongmin Liu[c]

[a]*State Key Laboratory of Molecular Reaction Dynamics, Dalian Institute of Chemical Physics, Chinese Academy of Sciences, Dalian 116023, PR China*
[b]*Division of Chemistry and Biological Chemistry, School of Physical and Mathematical Sciences, 637617 Singapore, Singapore*
[c]*State Key Laboratory of Catalysis, Dalian Institute of Chemical Physics, Chinese Academy of Sciences, Dalian 116023, PR China*

Received 18 June 2007; received in revised form 23 August 2007; accepted 23 August 2007
Available online 18 October 2007

Abstract

The coordination of extra-framework Li^+ in faujasite (FAU) and the interaction between H_2 and Li-FAU were studied by the generalized-gradient approximation (GGA) of density functional theory (DFT) with the Perdew–Burke–Ernzerhof (PBE) exchange-correction functional. Four adsorption sites have been found to be stable for Li^+: site SI′, the most stable one, in the sodalite cage; site SII in the six-ring windows of the sodalite unit and sites SIII and SIII′ in the supercage. Hydrogen interacting with these sites prefers the side-on coordination geometry. Calculated adsorption energies decrease in the sequence of SIII′ > SIII > SI′ > SII, consistent with the calculated Li–H distance and the charge on H_2. The H–H stretching frequencies of adsorbed species at 4286–4346 cm^{-1} are by about 7–67 cm^{-1} lower than in the free hydrogen molecules. The small bathochromic harmonic H_2 frequency shift is in agreement with the small H_2 bond elongation.

Keywords: DFT; Hydrogen adsorption; Zeolite; FAU

1. Introduction

In the approach to a viable hydrogen-based economy, the safe and affordable for storage of hydrogen still presents a challenging issue [1]. Among the different storage methods [2–6], adsorption on materials presents the advantage of simplicity and of quick kinetics of the charge and discharge cycles. Concerning sorbent materials, zeolites have been the major candidates for hydrogen storage due to their high thermal stability, low cost, high bulk density, and adjustable composition. It has been reported that the amount of hydrogen adsorbed on zeolites depends on the framework structure, composition, and also acidic–basic nature of the zeolites [7,8]. It is known that cations in the zeolite create strong electric fields that will favor gas adsorption [4]. So far, there are many experimental and theoretical studies with the hydrogen molecule interacting with different kinds of cations in various zeolites [9–13].

Here we report the hydrogen adsorption in the zeolite Li-FAU. FAU has been selected because it seems to be a suitable zeolitic framework type for hydrogen purification and adsorption. The FAU structure consists of sodalite cages (truncated cuboctahedra) linked by double six-rings (D6Rs) as shown in Fig. 1. The sodalite cage and D6Rs are applied as encapsulation materials for H_2 because they contain a maximum pore opening with a size similar to that of the kinetic diameter of molecular hydrogen, 2.89 Å. For commercial applications, a hydrogen storage tank should be able to efficiently store a sufficient amount of hydrogen with acceptable weight proportions [14]. This is the first reason for us choosing Li^+; its light mass (6 protons mass) is significantly smaller than that for other cations such as Na^+ (22 protons mass), or Cu^+ (58 protons mass). For the second reason is that large size of alkali metal cations' presence may affect the available void volume, thus limiting the pore space for hydrogen adsorption. It is worth noting that Li-LSX has a hydrogen storage capacity of 0.6 wt%, among the highest for allknown sorbent materials at ambient temperature [7].

2. Computational details

All the cluster calculations were performed with density functional theory (DFT) within the generalized-gradient approximation (GGA) approximations using $DMol^3$ code of

* Corresponding author. Tel.: +86 411 84379293; fax: +86 411 84675584.
E-mail address: klhan@dicp.ac.cn (K. Han).

0360-3199/$ - see front matter © 2007 International Association for Hydrogen Energy. Published by Elsevier Ltd. All rights reserved.
doi:10.1016/j.ijhydene.2007.08.027

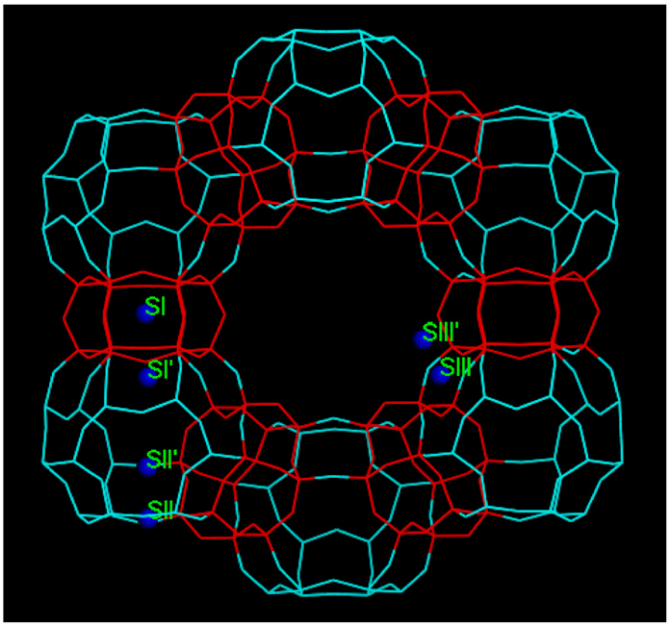

Fig. 1. FAU structure with extraframework cation sites denoted. Sitting sites of cations (SI, SI′, SII, SII′, SIII, and SIII′) as yellow spheres. For the sake of clarity, the D6Rs units are red; the sodalite cages are light blue.

Accelrys Inc. [15]. The Perdew–Burke–Ernzerhof (PBE) exchange-correction functional [16,17] and the double numerical plus polarization (DNP) [18–20] basis set, which is equivalent in accuracy to the commonly used 6-31G** Gaussian orbital basis set, were used throughout the calculations. However, the numerical basis set is much more accurate than a Gaussian basis set with the same size. More recently, van den Berg and co-workers have found that the GGA with the PBE functional can give an accurate account of the H_2–H_2 interactions within confined $(H_2)_N$ clusters [21]. Each basis function was restricted to within a cutoff radius of $R_{cut} = 5.0$ Å, while the convergence criteria were set as follows: energy $= 2 \times 10^{-5}$ Ha; force $= 4 \times 10^{-3}$ Ha/Å; displacement $= 0.005$ Å. Thereby, allowing for efficient calculations without a significant loss of accuracy.

The cluster we choose consists of a sodalite cage and D6Rs, which extend the study by a large series of bare extraframework cations or the clusters limited to S6Rs (a single six-membered ring) or D6Rs [22–24]. One framework Si atom was replaced by aluminium and the charge was compensated for by a Li^+ cation. In these models, the dangling bonds of the Si atoms are terminated by H atoms and the Si–H bonds are oriented along the bond direction to what would otherwise have been the next oxygen atom. By doing this we are aware that our model will miss some of the details of the cation–framework interaction. Our strategy is first to provide a certain basic understanding in the simplest cases. More sophisticated models will be developed in the future in order to predict cation distributions more accurately. Full structure optimization of the clusters representing the various sorption complexes was performed without geometry restrictions or fixed coordinates.

To test the accuracy of DMol^3 in describing H-bond strengths, the interaction energies between two water molecules were computed using the PBE/DNP/$R_{cut} = 5.0$ Å settings, as described in the previous section. The calculated value of 4.7 kcal/mol compares well with experimentally estimated ranges of 4.7–6.1 kcal/mol [25]. The standard procedure in ab initio calculations of interaction energies uses the so-called basis set superposition error (BSSE) approach [26] to account for incomplete atomic basis sets. The DMol^3 program uses numerical functions that are far more complete than the traditional Gaussian functions. Moreover, this basis set is known to produce a small BSSE [27,28]. Considering both the size of the model and the level of calculation method, we are convinced that the conclusions that will be drawn in the following should be quite reliable.

3. Results and discussion

3.1. Li^+ sites in FAU

In order to study the substitution of Si^{4+} by (Al^{3+}, Li^+), we replaced a Si^{4+} in a T site by an Al^{3+} and introduced a Li^+ to compensate the charge on the framework created by an Al/Si substitution. Fig. 1 shows the six possible sitting sites of Li^+ in the FAU zeolite. Even if all of them have been considered in the calculations, only parts of the sites have been found to be stable for the Li^+. For the SI, and SII′ sites, geometry optimization brings the Li^+ into the site SI′. It is impossible to present the entire trajectory for the motions here and, instead, selected representative angle (Al–Li–Si) versus optimized step is presented in Fig. 2. One can clearly see that the Li cation in SI and SII′ sites transferred to the SI′ site. The selected bond distances and angles and the relative stability are reported in Table 1. Also shown in Table 1 for comparison are the results of experimental [29–31] and similar calculations with D6Rs [24] reported in the literature. It shows that the distance between the bridging oxygen and Li atom (R(Li–O)) of the present work has a better match to experiment than that in the D6Rs simulation. The angle of O–Li–O is in reasonable agreement with the experimental data. Therefore, we can conclude that clusters we used in the work are adequate to represent the interaction of H_2 and the acid sites in zeolite framework. From the relative stability of the Li^+ sitting sites in the Table 1, we found that site SI′ turned out to be the most stable location for Li^+, which is in agreement with the study by D6Rs [24]. The SII′ site is preferred next and then follows the SIII′ site. The last is SIII site. The present results can be compared with other experimental reports. According to Plevert et al. [31], sites SI′ and SII′ are fully occupied, and the Li^+ in a supercage are equally distributed between SIII and SIII′ sites. In a dehydrated zeolite, the SIII′ cations can be regarded as nearly “bare”: they should be easily accessible and have high adsorption capacity. This preliminary step allowed us to validate the choice of the cluster size and method used in the calculations.

3.2. H_2 interaction with Li-FAU

In order to investigate the cationic effect on the interaction of sorbates in the Li-FAU/H_2, the naked Li/H_2 adducts have

also been performed and compared. The coordination of H_2 molecule adsorption can take place through two possible structures: the side-on [14,32] and the end-on structures (Scheme 1). The end-on structures are not stable: geometry optimization brings the end-on structure to the side-on structure, except for the naked Li cation. For naked Li cation, the adsorption energy with the side-on structure is considerably more compared to the end-on structure and shows the closest agreement with the literature data [11]. So, we can say that the H_2 molecule mainly interacts with an active site via the bonding electron density accumulated between the two H atoms, that is, the side-on structure, in agreement with the literature [32].

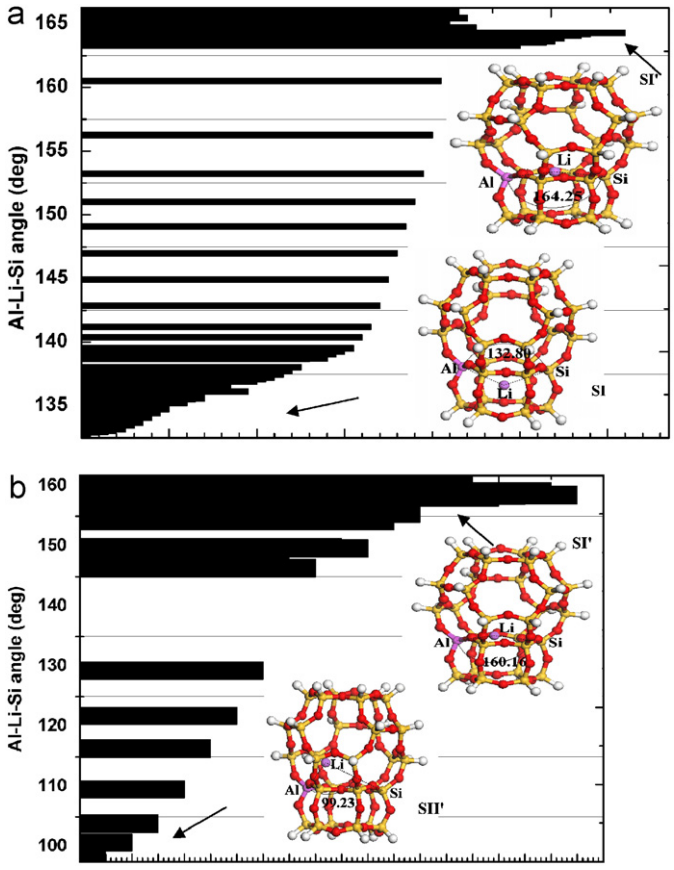

Fig. 2. Angle distribution of the Al–Li–Si for optimizing the Li cation in the (a) SI site, (b) SII′ site. The Si atom is at the next-next-nearest-neighbor (NNNN) site in the S6Rs.

Selected optimized geometrical structures for H_2 adsorption on Li-FAU and the H_2 adsorption energy, as well as the Mulliken population analysis are documented in Table 2. The interaction of H_2 with the "bare" cation Li^+ is considerably stronger compared to the interaction of H_2 with Li^+ embedded in a zeolite environment, as shown in Table 2. Fig. 3 shows the optimized geometries for the H_2 adsorption on Li-FAU. The Li–H internuclear distances for the "bare" Li^+ adsorption complexes Li/H_2 are shorter, the adsorption energies considerably are higher and the adsorbate molecule polarization is very strong. For Li^+ there is a clear dependence on the cation site: the weakest adsorption is for Li^+ in the SII site, where it is embedded in the six-ring. Here, the hydrogen cannot approach the cation as closely as for all other sites. Therefore, the lower interaction energy at the SII site compared to the other sites is due to extra repulsion between the hydrogen molecule and the rest of the framework [33]. This result agrees with previous Monte Carlo studies, according to which, Li^+ cations at SII sites are not involved in the adsorption process [34]. The comparison of the H_2 adsorption energies clearly shows that the SIII site and SIII′ site, which are in the supercage, are more favorable than the SI′ and SII sites (Table 2). The Li^+ cation at SIII′ site has a much higher H_2 adsorption energy (12.15 kJ/mol), as compared to all other sites under study.

We can observe that the Li–H distances for H_2 bonding to Li^+ decrease in the order: SIII′ < SI′ < SIII < SII, which correlate with the adsorption energy. The closer the hydrogen approaches the extra-framework cation, the stronger the interaction becomes. The adsorption energy is inversely proportional to the stability of the site. This trend is consistent with those previously reported from experimental and theoretical results for the adsorption of H_2 in metal-exchanged ferrierite [35], MOR [36], FER [11,37] or other gases in various zeolite systems [38–42]. The more tightly the extra-framework cation binds to the zeolite framework, the lower the adsorption strength of the

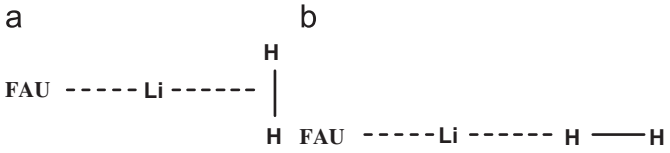

Scheme 1. Schematic representation of the interaction of H_2 with Li^+: (a) side-on; (b) end-on.

Table 1
Relative stability E_{rel}(kcal/mol) of the metal cations sitting site and simulated structural data

Site	Stabilization energy (kcal/mol)	R(Li–O) (Å)			O–Li–O (deg)	
		Present work	Expt.	D6Rs [24]	Present work	Expt.
SI	SI′					
SI′	0	1.915	1.902 [29,30]	1.985	112.23	118.5 [31]
SII	1.32	1.913	1.930 [42]	2.050	112.224	120.0 [31]
SII′	SI′					
SIII	21.44	1.999	2.010 [31]		106.715	
SIII′	12.45	1.858	1.880 [31]	1.801	89.740	

Table 2
Geometry of the adsorption complex of H_2 on Li^+-FAU, Mulliken population analysis (electrons) and adsorption energies

Cluster model/H_2 + Li(Z)	R_{Li-H} (Å)	R_{H-H} (Å)	Δv^a(cm^{-1})	q (H_2)	ΔE^0 (kJ/mol)
Naked Li^+	2.029 (2.026 [11])	0.755 (0.761 [11])	−67	0.172	25.03 (23.5 [11])
Naked Li^{+b}	2.059	0.751	−7	0.072	8.12
Li^+ at SI′	2.308	0.753	−20	0.065	8.97
Li^+ at SII	2.526	0.753	−40	0.048	5.90
Li^+ at SIII	2.177	0.753	−13	0.075	11.69
Li^+ at SIII′	2.097	0.754	−65	0.084	12.15

[a] Δv is the shift in harmonic stretching frequency of hydrogen with respect to the free molecule.
[b] The end-on structure.

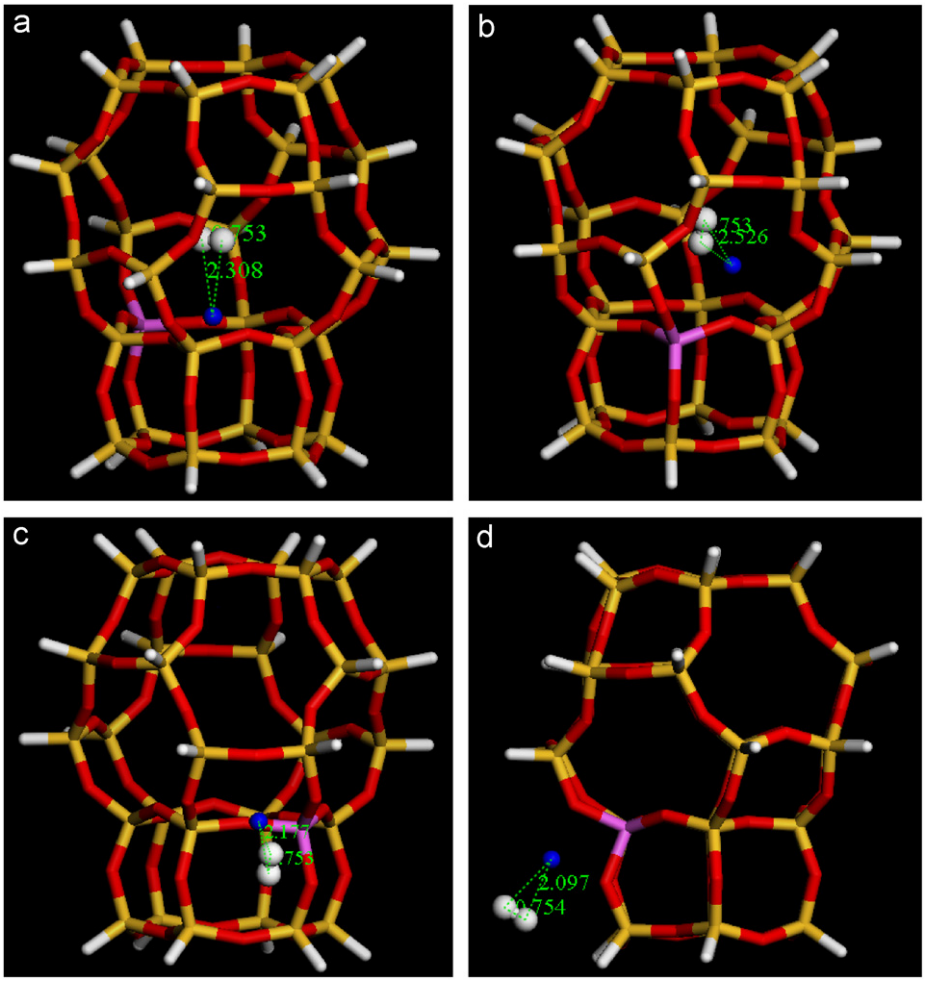

Fig. 3. Optimized geometry of the H_2 molecule adsorbed on the (a) SI′ site (b) SII site (c) SIII site and (d) SIII′ site. The color code is as follows: white, hydrogen; blue, Li cation; red, oxygen; yellow, silicon, and pink, aluminum. Bond distances in Å.

cation is. As pointed out above, here we find that the adsorption energy decreases with increasing the Li–H distance.

The increase of the bond length of H_2 induced by the adsorption on the Lewis acid site in the zeolite represents an activation of the adsorbed molecule. Only a small degree of bond activation is observed for these sites, indicating a nonchemical interaction [43]. The H–H bond length varies by −0.001–0.003 Å in the adsorption complexes; only the interaction with "bare" Li^+ leads to an increase of the H–H length by 0.003 Å. The charge transfer from the H_2 molecule to the cation has been evaluated by means of the hydrogen charge after the adsorption. It is well known that the increase of the charge on the hydrogen (qH_2) corresponds to the increase of the electron transference, and thus, to the increase of the Lewis acid site. So it can be stated from the qH_2 data listed in Table 2 that the acid strength of the Li-FAU sites increases in the order of SII < SI′ < SIII < SIII′, which shows a high consistency with the calculated adsorption energy, the geometric parameters.

The bond activation of the adsorbed H_2 molecule leads to the downshift of the intramolecular stretching frequency. The stretching frequency of the free molecule is 4353 cm^{-1}. This results in a significant overestimation of the experimental frequency by 192 cm^{-1} [44], which in turn leads to an underestimation of the previous theoretical frequency by 31 cm^{-1} [12]. The discrepancy originates in the exchange-correlation functional. Because the GGA functional [45] overestimates the bond strength of H_2, the frequency is higher than that experimentally observed [12,44]. H–H stretching frequencies of adsorbed species at 4286–4346 cm^{-1} are by about 7–67 cm^{-1} lower than those in the free hydrogen molecules. The small bathochromic shift (see Table 2) in H–H stretching frequency is in agreement with the small H_2 bond elongation.

4. Conclusion

The adsorption of hydrogen on Li-FAU zeolite has been investigated by means of density functional theory. DFT studies reveal that Li^+ strongly prefers the SI′ sites in the sodalite. The coordination of H_2 prefers the side-on structure. The Li^+ cations at SIII′ sites have the highest adsorption energy among the examined sites. By analyzing the adsorption energy, the geometric parameters, and the charge on the H_2, we concluded that the acidity of the Li-FAU sites decreases in the order of SIII′ > SIII > SI′ > SII. The vibrational frequency of the H–H stretching mode of the H_2 molecule adsorbed in the cluster was redshifted from that in free molecule. The small bathochromic shift in H–H stretching frequency is in agreement with the small H_2 bond elongation.

Acknowledgments

This work was supported by NSFC (20573110). KLH is a member of Virtual Laboratory for Computational Chemistry, CNIC, CAS.

References

[1] Alper J. Water splitting goes au naturel. Science 2003;299:1686–7.
[2] Syed MT, Sherif SA, Veziro Lu TN, Sheffield JW. An economic analysis of three hydrogen liquefaction systems. Int J Hydrogen Energy 1998;23:565–76.
[3] Sandrock G, Bowman RC. Gas-based hydride applications: recent progress and future needs. J Alloy Compd 2003;356:794–9.
[4] Sandrock G. A panoramic overview of hydrogen storage alloys from a gas reaction point of view. J Alloy Compd 1999;293:877–88.
[5] Zuttel A. Materials for hydrogen storage. Mater Today 2003;6:24–33.
[6] Liu YF, Hu JJ, Xiong ZT, Wu GT, Chen P, Murata K. et al. Investigation on hydrogen desorption from the mixture of $Mg(NH_2)_2$ and CaH_2. J Alloy Compd 2007;432:298–302.
[7] Li YW, Yang RT. Hydrogen storage in low silica type X zeolites. J Phys Chem B 2006;110:17175–81.
[8] Weitkamp J, Fritz M, Ernst S. Zeolites as media for hydrogen storage. Int J Hydrogen Energy 1995;20:967–70.
[9] Otero Areán C, Manoilova OV, Bonelli B, Rodríguez Delgado M, Turnes Palomino G, Garrone E. Thermodynamics of hydrogen adsorption on the zeolite Li-ZSM-5. Chem Phys Lett 2003;370:631–5.
[10] Solans-Monfort X, Branchadell V, Sodupe M, Zicovich-Wilson CM, Gribov E, Spoto G. et al. Can Cu^+-exchanged zeolites store molecular hydrogen? An ab-initio periodic study compared with low-temperature FTIR. J Phys Chem B 2004;108:8278–86.
[11] Nachtigall P, Garrone E, Turnes Palomino G, Rodríguez Delgado M, Nachtigallová D, Otero Areán C. FTIR spectroscopic and computational studies on hydrogen adsorption on the zeolite Li-FER. Phys Chem Chem Phys 2006;8:2286–92.
[12] Beno L, Bucho T, Hafner J, Toulhoat H. A density functional theory study of molecular and dissociative adsorption of H_2 on active sites in mordenite. J Phys Chem B 2005;109:22491–501.
[13] Torres FJ, Civalleri B, Terentyev A, Ugliengo P, Pisani C. Theoretical study of molecular hydrogen adsorption in Mg-exchanged chabazite. J Phys Chem C 2007;111:1871–3.
[14] van den Berg AWC, Bromley ST, Jansen JC. Thermodynamic limits on hydrogen storage in sodalite framework materials: a molecular mechanics investigation. Microporous Mesoporous Mater 2005;78:63–71.
[15] DMol3, Materials Studio version 3.1 from Accelrys: ⟨http://www.accelrys.com/mstudio/dmol3.html⟩.
[16] Perdew JP, Burke K, Ernzerhof M. Generalized gradient approximation made simple. Phys Rev Lett 1996;77:3865–8.
[17] Perdew JP, Burke K, Ernzerhof M. Generalized gradient approximation made simple (vol. 77, p. 3865, 1996). Phys Rev Lett 1997;78:1396.
[18] Delley B. An all-electron numerical method for solving the local density functional for polyatomic molecules. J Chem Phys 1990;92:508–17.
[19] Delley B. Fast calculation of electrostatics in crystals and large molecules. J Phys Chem 1996;100:6107–10.
[20] Delley B. From molecules to solids with the $DMol^3$ approach. J Chem Phys 2000;113:7756–64.
[21] van den Berg AWC, Bromley ST, Wojdel JC, Jansen JC. Molecular hydrogen confined within nanoporous framework materials: comparison of density functional and classical force-field descriptions. Phys Rev B 2005;72:155428–34.
[22] Tugsuz T, Dogan M, Sevin F. A theoretical study on the location of Ni^{2+}, Cu^{2+}, Cr^{2+}, Cd^{2+} and Pb^{2+} in zeolite Y. J Mol Struct (THEOCHEM) 2005;728:103–9.
[23] Mikosch H, Uzunova EL, Nikolov GS. Interaction of molecular nitrogen and oxygen with extraframework cations in zeolites with double six-membered rings of oxygen-bridged silicon and aluminum atoms: a DFT study. J Phys Chem B 2005;109:11119–25.
[24] Uzunova EL, Mikosch H. Electronic structure and stability of double six-membered rings of oxygen-bridged silicon and aluminum atoms related to cation site occupancy in FAU zeolites: a DFT study. J Phys Chem B 2004;108:6981–7.
[25] Novoa JJ, Sosa C. Evaluation of the density functional approximation on the computation of hydrogen bond interactions. J Phys Chem 1995;99:15837–49.
[26] Szalewicz K, Jeziorski B. In: Scheiner S, editor. Molecular interactions. New York: Wiley; 1997. p. 3.
[27] Andzelm J, Govind N, Fitzgerald G, Maiti A. DFT study of methanol conversion to hydrocarbon in a zeolite catalyst. Int J Quant Chem 2003;91:467–73.
[28] Govind N, Andzelm J, Reindel K, Fitzgerald G. Zeolite-catalyzed hydrogen formation from methanol: density functional simulations. Int J Mol Sci 2002;3:423–34.
[29] Feuerstein M, Lobo RF. Characterization of Li cations in zeolite LiX by solid-state NMR spectroscopy and neutron diffraction. Chem Mater 1998;10:2197–204.
[30] Feuerstein M, Lobo RF. Influence of oxygen and nitrogen on ^7Li MAS NMR spectra of zeolite LiX-1.0. Chem Commun 1998;16:1647–8.
[31] Plevert J, Di Renzo F, Fajula F, Chiari G. Structure of dehydrated zeolite Li-LSX by neutron diffraction: evidence for a low-temperature orthorhombic faujasite. J Phys Chem B 1997;101:10340–6.
[32] Vitillo JG, Damin A, Zecchina A, Ricchiardi G. Theoretical characterization of dihydrogen adducts with alkaline cations. J Chem Phys 2005;122:114311–20.
[33] Plant DF, Simperler A, Bell RG. Adsorption of methanol on zeolites X and Y. An atomistic and quantum chemical study. J Phys Chem B 2006;110:6170–8.

[34] Jale SR, Bülow M, Fitch FR, Perelman N, Shen D. Monte Carlo simulation of sorption equilibria for nitrogen and oxygen on LiLSX zeolite. J Phys Chem B 2000;104:5272–80.

[35] Bordiga S, TurnesPalomino G, Pazè C, Zecchina A. Vibrational spectroscopy of H_2, N_2, CO and NO adsorbed on H, Li, Na, K-exchanged ferrierite. Microporous Mesoporous Mater 2000;34:67–80.

[36] Benco L, Bucko T, Hafner JH, Toulhoat H. Periodic DFT calculations of the stability of Al/Si substitutions and extraframework Zn^{2+} cations in mordenite and reaction pathway for the dissociation of H_2 and CH_4. J Phys Chem B 2005;109:20361–9.

[37] Otero Areán C, Turnes Palomino G, Garrone E, Nachtigallová D, Nachtigall P. Combined theoretical and FTIR spectroscopic studies on hydrogen adsorption on the zeolites Na-FER and K-FER. J Phys Chem B 2006;110:395–402.

[38] Chandrakumar KRS, Pal S. DFT and local reactivity descriptor studies on the nitrogen sorption selectivity from air by sodium and calcium exchanged zeolite-A. Collids Surf A 2002;205:127–38.

[39] Nachtigall P, Bulánek R. Theoretical investigation of site-specific characteristics of CO adsorption complexes in the Li^+-FER zeolite. Appl Catal A Gen 2006;307:118–27.

[40] Limtrakul J, Jungsuttiwong S, Khongpracha P. Adsorption of carbon monoxide on H-FAU and Li-FAU zeolites: an embedded cluster approach. J Mol Struct 2000;525:153–62.

[41] Limtrakul J, Khongpracha P, Jungsuttiwong S, Truong TN. Adsorption of carbon monoxide in H-ZSM-5 and Li-ZSM-5 zeolites: an embedded ab initio cluster study. J Mol Catal A Chem 2000;153:155–63.

[42] Plant DF, Maurin G, Deroche I, Gaberova L, Llewellyn PL. CO_2 adsorption in alkali cation exchanged Y faujasites: a quantum chemical study compared to experiments. Chem Phys Lett 2006;426:387–92.

[43] Lochan RC, Head-Gordon M. Computational studies of molecular hydrogen binding affinities: the role of dispersion forces, electrostatics, and orbital interactions. Phys Chem Phys Chem 2006;8:1357–70.

[44] Stoicheff BP. High resolution raman spectroscopy of gases .9. Spectra of H_2, HD, and D_2. Can J Phys 1957;35:730–41.

[45] Perdew JP, Chevary A, Vosko SH, Jackson KA, Pedersen MR, Singh DJ. et al. Atoms, molecules, solids, and surfaces: applications of the generalized gradient approximation for exchange and correlation. Phys Rev B 1992;46:6671–87.